Available online at www.sciencedirect.com
ScienceDirect
Biochimica et Biophysica Acta 1768 (2007) 538–552
Biochimica et Biophysica Acta
BBA
www.elsevier.com/locate/bbamem

The predicted transmembrane fragment 17 of the human multidrug resistance protein 1 (MRP1) behaves as an interfacial helix in membrane mimics

Michel Vincent [a,b], Jacques Gallay [a,b], Nadège Jamin [c], Manuel Garrigos [c], Béatrice de Foresta [c,*]

[a] CNRS UMR8619 IBBMC, Orsay, F-91405, France
[b] Univ Paris-Sud, Orsay, F-91405, France
[c] Section de Biophysique des Fonctions Membranaires, DBJC et CNRS URA 2096, CEA Saclay, 91191, Gif sur Yvette cedex, France

Received 27 July 2006; received in revised form 9 November 2006; accepted 29 November 2006
Available online 16 December 2006

Abstract

The human multidrug resistance protein MRP1 (or ABCC1) is one of the most important members of the large ABC transporter family, in terms of both its biological (tissue defense) and pharmacological functions. Many studies have investigated the function of MRP1, but structural data remain scarce for this protein. We investigated the structure and dynamics of predicted transmembrane fragment 17 (TM17, from Ala_{1227} to Ser_{1251}), which contains a single Trp residue (W_{1246}) involved in MRP1 substrate specificity and transport function. We synthesized TM17 and a modified peptide in which Ala_{1227} was replaced by a charged Lys residue. Both peptides were readily solubilized in dodecylmaltoside (DM) or dodecylphosphocholine (DPC) micelles, as membrane mimics. The interaction of these peptides with DM or DPC micelles was studied by steady-state and time-resolved Trp fluorescence spectroscopy, including experiments in which Trp was quenched by acrylamide or by two brominated analogs of DM. The secondary structure of these peptides was determined by circular dichroism. Overall, the results obtained indicated significant structuring (~50% α-helix) of TM17 in the presence of either DM or DPC micelles as compared to buffer. A main interfacial location of TM17 is proposed, based on significant accessibility of Trp_{1246} to brominated alkyl chains of DM and/or acrylamide. The comparison of various fluorescence parameters including λ_{max}, lifetime distributions and Trp rotational mobility with those determined for model fluorescent transmembrane helices in the same detergents is also consistent with the interfacial location of TM17. We therefore suggest that TM17 intrinsic properties may be insufficient for its transmembrane insertion as proposed by the MRP1 consensus topological model. This insertion may also be controlled by additional constraints such as interactions with other TM domains and its position in the protein sequence. The particular pattern of behavior of this predicted transmembrane peptide may be the hallmark of a fragment involved in substrate transport.

Keywords: MRP1 (ABCC1) transmembrane helix 17; Aromatic residues; Steady-state and time-resolved fluorescence; Brominated detergents; Dodecylmaltoside and dodecylphosphocholine micelles; Multidrug resistance

1. Introduction

The human multidrug resistance-associated protein (MRP1) was discovered in 1992 [1] and has since been identified as a potential therapeutic target. MRP1 belongs to the large family of ATP-binding cassette (ABC) transport proteins. It is the representative of the ABCC branch of this family, 13 members of which have been identified to date (http://www.nutrigene.4t.com/humanabc.htm), and is also known as ABCC1. It is present in most tissues and functions as an ATP-driven transporter that expels various structurally unrelated molecules, including various xenobiotics and amphiphilic organic anions such as glutathione (GSH)-, glucuronate- and sulfate-conjugated compounds, from

Abbreviations: MRP1 (or ABCC1), multidrug resistance protein 1; LTC_4, cysteinyl leukotriene C_4; $E_2$17βG, estradiol 17-(β-D-glucuronide); GSH, reduced glutathione; DM, dodecylmaltoside; BrDM, 7, 8-dibromododecylmaltoside; BrUM, 10, 11-dibromoundecanoylmaltoside; DPC, dodecylphosphocholine; NATA, N-acetyltryptophanamide; TOE, tryptophan octyl ester; DMSO, dimethylsulfoxide; MSD, membrane-spanning domain; TM, transmembrane; MEM, maximum entropy method; P3, $K_2WL_9AL_9K_2A$; P5, $K_2CLWL_7AL_9K_2A$; P7, $K_2CL_3WL_5AL_9K_2A$; P9, $K_2CL_5WL_3AL_9K_2A$; P11, $K_2CL_7WLAL_9K_2A$; P13, $K_2CL_9WL_9K_2A$; TM17, AGL-VGL-SVS-YSL-QVT-TYL-NWL-VRM-S; mTM17, KGL-VGL-SVS-YSL-QVT-TYL-NWL-VRM-S

* Corresponding author. Fax : +33 1 69088139.
E-mail address: beatrice.de-foresta@cea.fr (B. de Foresta).

0005-2736/$ - see front matter © 2006 Elsevier B.V. All rights reserved.
doi:10.1016/j.bbamem.2006.11.021

the cell [2]. MRP1 also transports unconjugated drugs in the presence of GSH, possibly as a cotransporter [3,4]. MRP1 overexpression confers multidrug resistance on tumor cells and, in some hematological cancers, such as acute leukemia, it seems to be associated with a poor response to chemotherapy [5]. Furthermore, even in cells in which MRP1 is not overexpressed, this protein may affect the pharmacokinetic properties of drugs used for chemotherapy.

MRP1 is a large glycosylated integral membrane protein with an M_r of 190,000 (1531 residues) which, according to protein folding algorithms, contains three membrane-spanning domains (MSD). The current topological model, which is supported by epitope insertion [6,7] and glycosylation site mutation data [8], consists of a specific N-terminal domain, MSD0, preceded by an extracytosolic N-terminus and followed by a cytosolic loop (L0), and two membrane domains MSD1 and MSD2, each followed by a nucleotide-binding domain. Five transmembrane (TM) helices are predicted for MSD0 and six each for MSD1 and MSD2. However, experimental structural data remain scarce, despite detailed studies of the function of this protein.

Site-directed mutagenesis experiments investigating the 17 predicted TM helices have demonstrated the functional importance of fragment 17 (TM17), the most proximal helix of the cytoplasmic MRP1 C-terminus [9,10]. In particular, mutations in which Trp_{1246} was replaced by Cys, Ala, Phe, or Tyr abolished the transport of estradiol 17-(β-D-glucuronide), an endogenous estradiol metabolite formed in the liver and excreted into bile, and prevented the drug resistance mediated by MRP1 [10]. In addition, W1246 is conserved among the various homologs of MRP1 and it has been suggested that this residue forms a ring of functional importance with other aromatic residues (W553, F594, W1198 and Y1243), based on molecular modeling of MSD1 and 2 [11].

We investigated the topological organization and dynamics of TM17 in membrane mimetic systems, by means of Trp fluorescence and circular dichroism. W1246 is the only Trp residue in TM17, making therefore this fragment ideal for fluorescence experiments. This strategy, involving studies of an isolated TM fragment, was based on the notion that membrane proteins folding includes an initial formation of independently stable transmembrane helices before their association within the membrane—known as the two-stage model [12]. This model was recently refined to include an additional stage, in which helix association leads to further folding events, such as specific binding [13]. Initial events such as interfacial binding and folding of a TM fragment have also been rationalized from a thermodynamic viewpoint [14].

The TM17 fragment under study has the following amino-acid sequence:

$$A_{1227}GL-VGL-SVS-\mathbf{Y}_{1236}SL-QVT-T\mathbf{Y}_{1243}L-N\mathbf{W}_{1246}L-VRM-S_{1251}$$

where the residues are numbered according to their position in the protein, with aromatic residues shown in bold. It encompasses the TM17 sequence (G_{1228}–V_{1248}) predicted by the MEMSAT algorithm (e.g. [10]), with additional C-term amino-acids (of which the charged Arg_{1249}) critical for GSH-dependent binding of substrates and leukotriene C_4 (LTC_4) binding and transport [15,16]. Most of the experiments were also performed with the fragment:

$$K_{1227}GL-VGL-SVS-\mathbf{Y}SL-QVT-T\mathbf{Y}L-N\mathbf{W}L-VRM-S_{1251}$$

in which the N-terminal hydrophobic Ala was replaced by a charged Lys residue.

As previously (also see discussion below), we selected two of the most suitable detergents for membrane protein (or peptide) studies – dodecylmaltoside (DM) and dodecylphosphocholine (DPC) – to use their micelles as membrane mimics. DM in particular was the detergent in which MRP1 was recently purified close to homogeneity while retaining functional activity [15]. We applied a recently described method for topological studies, making use of previously synthesized brominated analogs of DM [17]. The use of brominated detergents makes it possible to detect Trp-detergent contacts by fluorescence analysis, because bromine atoms quench Trp residues with which they are in contact (or within a very short distance) with high efficiency, via the so-called heavy atom quenching mechanism [18,19].

The interaction of native and mutated TM17 fragments with micelles of DM and DPC was characterized using various fluorescence approaches. We analyzed the steady-state fluorescence spectra and decomposition of these spectra into their elementary components, to estimate the polarity of the Trp microenvironment. The depth-dependent fluorescence quenching of Trp by 7,8-dibromododecylmaltoside (BrDM) or 10,11-dibromoundecanoylmaltoside (BrUM) as brominated analogs of DM, or by acrylamide as a soluble quencher, enabled us to estimate the location of Trp in the micelle. Time-resolved fluorescence intensity and fluorescence anisotropy data provided information concerning Trp rotamer distribution and dynamics, respectively, in the subnanosecond and nanosecond time ranges. Secondary structure was deduced by analyzing far-UV CD spectra.

We also carried out steady-state and time-resolved fluorescence experiments for a set of fluorescent synthetic peptides in DPC micelles: the peptides used were Lys-flanked polyLeu sequences, which serve as models of transmembrane α-helices, each containing a single Trp (referred to as Pn, with *n* referring to the position of the Trp residue in the sequence). The results were used as a reference, extending the results previously obtained for these peptides in DM micelles [17].

2. Materials and methods

2.1. Chemicals

DM was obtained from Calbiochem and its two brominated derivatives – 7,8-dibromododecylmaltoside (BrDM) and 10,11-dibromoundecanoylmaltoside (BrUM) – were synthesized by Insavalor (Villeurbanne, France), as previously described [20,21]. DPC was obtained from Avanti Polar Lipids (AL, USA) or from Anatrace (OH, USA). Stock solutions of these detergents were prepared in Milli-Q water at concentrations of 20 and 200 mM. N-acetyltryptophanamide

(NATA) and acrylamide were purchased from Sigma-Aldrich. We made up a stock solution of 5 M acrylamide in water. Methanol, ethanol and DMSO were obtained from Merck (Uvasol quality). Buffers were filtered through Millex-HA filters (0.45 μM pore size; Millipore).

2.2. Peptides

The peptide AGL-VGL-SVS-YSL-QVT-TYL-NWL-VRM-S (Mw=2797) (subsequently referred to as TM17), which encompasses the predicted transmembrane fragment 17 of MRP1, and its N-terminal mutant A1227K (called mTM17) (Mw=2853), were synthesized by Jerini (Berlin, Germany). Note that the mutation was performed on the side opposite to that demonstrated to be associated with substrate binding. These peptides were acetylated at the N-terminus and amidated at the C-terminus. TM17 preparations were >80–85% pure, whereas mTM17 preparations were 80–90% pure, as estimated by matrix-assisted laser desorption ionization time-of-flight (MALDI/TOF) mass spectrometry. They were used as supplied.

The six synthetic model peptides – $K_2WL_9AL_9K_2A$ (P3), $K_2CLWL_7AL_9K_2A$ (P5), $K_2CL_3WL_5AL_9K_2A$ (P7), $K_2CL_5WL_3AL_9K_2A$ (P9), $K_2CL_7WLAL_9K_2A$ (P11) and $K_2CL_9WL_9K_2A$ (P13) – denoted Pn, with the index *n* indicating the position of the Trp residue, were purchased from Research Genetics (Huntsville, AL, USA), as previously described [17]. A new batch of P13 was also obtained from Epytop (France). Stock solutions (2 mM) of model peptides were made up in methanol.

2.3. MRP1 fragment solubilization assays and preparation of mixed peptide-detergent micelles

Unlike Pn model peptides, TM17 was not soluble in methanol and was therefore dissolved in DMSO to give a clear stock solution (1 mM). By contrast, mTM17, which contains two positively charged residues instead of one in TM17 (Arg_{1249}), was dissolved in methanol and stock solutions (1 mM) were therefore made up in this solvent.

Concentrations were checked by comparison with absorption spectra in these solvents. Each peptide contains one Trp and two Tyr residues, and the molar absorption coefficient was taken as $\varepsilon_{max}=8400\ M^{-1}\ cm^{-1}$ at the maximum wavelength (~282 nm), using $\varepsilon=5600\ M^{-1}\ cm^{-1}$ and $1400\ M^{-1}\ cm^{-1}$ for Trp and Tyr, respectively, at the maximum, as previously described [22]. This may have resulted in a slight overestimation of concentrations (~10%), as the molar absorption coefficients of both Tyr and Trp may be slightly higher in alcoholic solutions [23]. We checked, with mTM17, that maximal absorbance in DMSO was similar to that in methanol.

Unless otherwise stated, the mixed peptide-detergent micelles were prepared by adding an aliquot of the peptide stock solution to the aqueous buffer (usually 10 mM potassium phosphate buffer, pH 7.5, at 20 °C) supplemented with 4 mM detergent (DM, DPC or mixtures of DM with one of its brominated analogs), with a dilution factor of at least 100 and constant stirring. In these conditions, most of DM and its analogs are in their micellar form, due to their low critical micellar concentration (cmc) (170–180 μM, 220 μM and 320 μM respectively for DM, BrDM and BrUM [21,24]). For DPC, 2.9 mM (out of 4 mM) detergent is micellar (as the cmc of DPC=1.1 mM [25]).

Note: the absorption of brominated detergents contributed to the absorption in the 250–270 nm range of peptides in micelles (together with that resulting from slight diffusion from the micelles) as an absorption band centered on a wavelength close to 200 nm was observed (as previously described for other brominated compounds [26]).

2.4. Small unilamellar vesicle preparation and peptide incorporation

SUV were prepared from egg PC and egg PS (Avanti Polar Lipids, Alabaster, Al). Briefly, the chloroformic solution of phospholipids was evaporated under a stream of nitrogen and dried under vacuum for 2–3 h. The dry film was rehydrated in 10 mM potassium phosphate buffer, pH 7.5, vortexed and sonicated (Vibrator Cell, Sonics, Cn) with the microtip. The peptides were either added in buffer to preformed SUV or co-evaporated with phospholipids.

2.5. Absorption measurements

Absorption spectra were recorded on an HP8453 diode array spectrophotometer, with a thermostatically controlled sample holder (20 °C). The sample was continuously stirred in a 1-cm path length cuvette.

2.6. Steady-state fluorescence measurements

Fluorescence data were obtained on a Spex Fluorolog spectrofluorometer. The temperature in the cuvette was controlled with a thermostat and the sample was continuously stirred. We used standard quartz cuvettes (1×1 cm). Excitation spectra were corrected for the spectrum of the lamp and both excitation and emission spectra were corrected for fluctuations in lamp intensity (usually very small, <1%).

2.7. Spectral decomposition of steady-state fluorescence emission spectra

The steady-state fluorescence spectra were analyzed using up to three four-parameter log-normal functions (a skewed Gaussian equation) of the following form [27,28]:

$$I(\nu) = I_m \exp\{-(\ln 2/\ln^2\rho) \times \ln^2[(a-\nu)/(a-\nu_m)]\} (at\ \nu < a)$$

$$I(\nu) = 0\ (at\ \nu < a)$$

here, $I_m=I(\nu_m)$ is the maximal fluorescence intensity; ν_m is the wavenumber of the band maximum (peak); $\rho=(\nu_m-\nu_-)/(\nu_+-\nu_m)$ is the band asymmetry parameter; ν_+ and ν_- are the wavenumber positions of left and right half-maximal amplitudes; a is the function-limiting point: $a=\nu_m+$ FWHM $\rho/(\rho^2-1)$; the full width at half-maximum FWHM$=\nu_+-\nu_-$.

We fitted a linear combination of this analytical model to the emission spectra by the least squares regression method (KaleidaGraph, Synergy Software, PA). A good fit was ensured by minimization of the squared residuals.

2.8. Fluorescence quenching by brominated detergents

Fluorescence quenching experiments of MRP1 fragments in mixed micelles of DM with a brominated analog (BrDM or BrUM) were performed essentially as previously described [17]. Data were analyzed with a lattice model of quenching ([29,30], see also [31]). This model was originally designed to describe the quenching of membrane fluorophores (e.g. protein Trp) by spin-labeled or brominated phospholipids. It considers two populations of fluorophores: one completely inaccessible to the quencher and responsible for the residual fluorescence F_{min} (e.g. Trp embedded in a protein), and one in which each fluorophore has *n* neighbors (phospholipids) and for which fluorescence is completely quenched if one (or more) of these sites is (are) occupied by a modified phospholipid (corresponding to a quenching efficiency of 100% upon contact). It is thought that phospholipids do not change position during the lifetime of the fluorophore. If *X* is the molar fraction of quenchers in the membrane, then $(1-X)^n$ is the probability that none of the *n* sites is occupied by a quencher. The fluorescence ratio is therefore given by: $F/F_0=(1-F_{min}/F_0)(1-X)^n+F_{min}/F_0$. In a micellar environment, unlike in lipid bilayers, the "lattice parameter" *n* is not expected to give an exact determination of quenchers around Trp because, in addition to static quenching, some dynamic quenching occurs [17,21], and because the transverse inaccessibility of Trp is not taken into account directly in the model. This parameter *n* is, however, correlated to the accessibility of this residue to brominated alkyl chains. We used the set of six model peptides Pn with Trp at various positions in the sequence (positions 3, 5, 7, 9 and 13 in the 25-amino acid sequence) to establish calibration curves for *n* [17]. We used these data as a reference, for comparison with the results obtained.

2.9. Fluorescence quenching by acrylamide

Fluorescence was quenched with acrylamide essentially as previously described [32]. Peptide quenching was analyzed using the classical Stern–Volmer equation (see, for reviews, [33,34]):

$$F_0/F = 1 + K_{SV}[Q]$$

where F_0 and F are the fluorescence intensities in the absence and presence of quencher, respectively, K_{sv} is the Stern–Volmer quenching constant and [Q] is the quencher concentration. K_{sv} is related to the bimolecular quenching constant k_q by the following formula:

$$K_{SV} = k_q \tau_0$$

where τ_0 is the lifetime, in the absence of quencher, of the fluorophore.

For NATA, taken as a reference, we used the nonlinear Stern–Volmer equation:

$$F_0/F = (1 + K_{SV}[Q])expV[Q]$$

where V can be considered as a sphere of action around the fluorophore in which the presence of a quencher molecule results in instantaneous (static) quenching.

2.10. Time-resolved fluorescence measurements

Fluorescence intensity and anisotropy decays were measured by the time-correlated single-photon counting technique from the polarized $I_{vv}(t)$ and $I_{vh}(t)$ components. Most experiments were performed as previously described [35] using the synchrotron radiation machine Super-ACO (Anneau de Collision d'Orsay). Experiments with mTM17 were carried out similarly, except that a light-emitting diode (PLS 295, serial number PLS-8-2-237 from Picoquant, Berlin-Adlershof, Germany) (maximal emission at 298 nm) was used as an excitation source and that a Hamamatsu photomultiplier (model R3235-01) was used for detection. As previously, fluorescence intensity $I(t)$ and anisotropy decays $A(t)$ were analyzed as sums of 150 or 100 exponential terms, respectively, by the maximum entropy method (MEM) [36] according to the following equations:

$$I(t) = \sum \alpha_i \exp(-t/\tau_i)$$

where α_i is the normalized amplitude and τ the lifetime of intensity decay, and

$$A(t) = \sum \beta_i \exp(-t/\theta_i)$$

where β_i is the anisotropy and θ_i the rotational correlation time of anisotropy decay. In this second analysis, we assume that each lifetime τ_i is associated with all rotational correlation times θ_i.

We recall that MEM does not impose any particular number of significant parameters for the decay. The Skilling–Jaynes entropy S is subjected to a χ^2 constraint [37], to ensure that the recovered distribution was consistent with the data.

2.11. Circular dichroism

Far UV circular dichroism spectra were recorded on a Jobin Yvon CD6 spectrodichrograph calibrated with ammonium d-10 camphorsulfonate. Measurements were made at 20 °C, using 0.1 cm and 0.01 cm path length quartz cuvettes (Hellma) for 25 μM peptide in buffer, with or without 4 mM detergent, and 100 μM peptide in methanol, respectively. Spectra were recorded in the 185 to 260 nm wavelength range with 0.5 nm wavelength increments, 2 s integration time and 2 nm spectral bandwidth. Spectra were averaged over four scans and corrected for background. Unsmoothed spectra are presented. The α-helical content of the peptides was initially estimated as for the model peptides [17] from the molar ellipticity value at 222 nm, $[\theta]_{222nm}$, taking into account an helix length-dependent factor according to [38]. Secondary structure was analyzed further with CDPro software (http://www.lamar.colostate.edu/~sreeram/CDPro) [39], which includes three different methods for analyzing protein CD spectra (CONTIN/LL, CDSSTR and SELCON3- [39,40]) and two reference protein sets, SDP42 (42 proteins) and SMP50 (50 proteins including 13 membrane proteins). CONTIN/LL and CDSSTR gave the most reliable analysis, as shown by the NRMSD (normalized root mean square deviation) and comparison of the plots of calculated and experimental spectra. We therefore used these two analyses to obtain a consensus estimate of secondary structure.

2.12. Calculation of the theoretical micellar rotational correlation time

Theoretical θ values were estimated as previously, assuming spherical micelles (so that $\theta = \eta V/RT$) and without taking into account micelle hydration. With n, the aggregation number of the micelles of 55 and 125 (±10%) respectively for DPC and DM, we obtained $\theta = 7.4$ ns for DPC and $\theta = 21$ ns for DM micelles, at 20 °C [41].

3. Results

3.1. Steady-state fluorescence spectra of TM17 and mTM17 in DM and DPC

Fig. 1A shows the fluorescence emission spectrum of the TM17 fragment diluted in an excess of DM or DPC micelles in 10 mM potassium phosphate buffer. In these conditions, TM17 readily interacts with the detergent micelles resulting in a fluorescence signal stable with time and with no significant

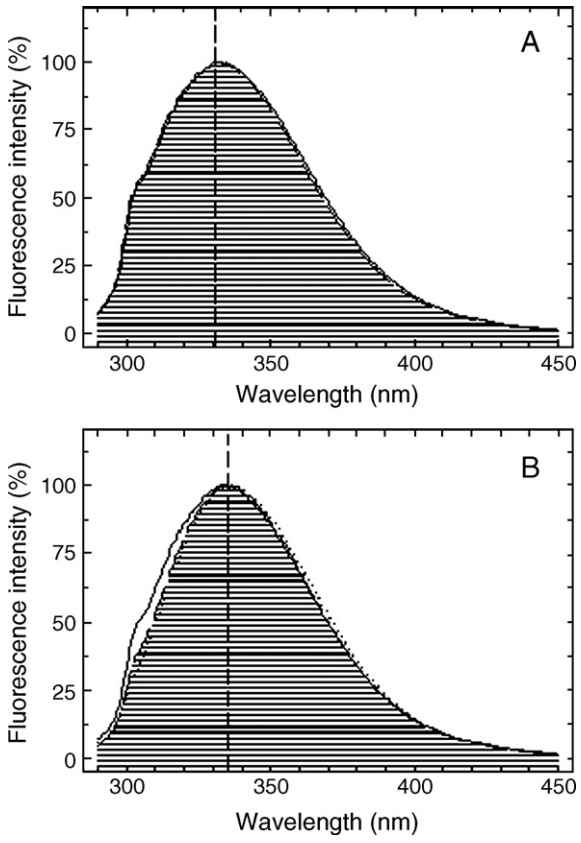

Fig. 1. Fluorescence emission spectra of TM17 and mTM17 in various media. (A) Normalized emission spectra of TM17 (5 μM) in 10 mM potassium phosphate buffer, pH 7.5, supplemented with 4 mM DM (continuous line) or 4 mM DPC (dashed line and hatched area) at 20 °C. λ_{ex} was set at 280 nm. Slit widths were 1.25 mm (bandwidths ~5 nm) for both excitation and emission. Spectra were recorded after a short period of equilibration (2–3 min) and the readings for background spectra (detergent in buffer) were subtracted. The vertical dashed line indicates λ_{max} in DPC. (B) Normalized emission spectra of mTM17 (5 μM) in the presence of 4 mM DM (same buffer as above) (continuous line) or 4 mM DPC (dashed line and hatched area) or mTM17 (10 μM) in methanol (dotted line), at 20 °C. Other conditions were as stated above.

fluctuations. The emission spectra of TM17 in the two detergents were almost entirely superimposable, indicating that the Trp residue was located in environments of similar average polarity in the two detergents. The emission maximum, λ_{max}, occurs at a value of 332 nm (Fig. 1A). This value indicates that the Trp is partially shielded from the bulk solvent (for NATA, a model for an exposed Trp, λ_{max}=353 nm). However, this value is slightly greater than the λ_{max} previously obtained for the single tryptophan-containing transmembrane model peptides P3, P5 and P7 in each detergent – ~327 nm in DM [17] and ~329 nm in DPC (see below) – suggesting that the Trp microenvironment is slightly more polar in TM17. In DMSO, the solvent in which the TM17 stock solution was prepared, λ_{max} was 338 nm, characteristic of a Trp residue fully exposed to this solvent, as expected (data not shown).

The emission spectrum of the N-terminal mutant mTM17 in 4 mM DM (Fig. 1B) was rather similar to that of TM17 in DM (with λ_{max} at 332 nm). By contrast, when mTM17 was diluted in DPC, its emission spectrum displayed a slight red shift, with λ_{max}=335 nm, suggesting a slightly more polar Trp environment. In methanol, the solvent for mTM17 stock solution, λ_{max} for mTM17 was 337 nm, as previously reported for the Pn model peptides, characteristic of a Trp exposed to this solvent.

These spectra were analyzed further by decomposition into their elemental components, using log-normal Gaussian distributions. This formalism suitable for fluorescence spectroscopy [28] originates from that developed for absorption spectroscopy [42]. This decomposition is illustrated for mTM17 in Fig. 2 and the parameters of the log-normal Gaussian curves are shown in Table 1 for both TM17 and mTM17. In pure solvents (methanol (Fig. 2C) or DMSO), a single main Gaussian curve accounted for Trp fluorescence, as expected for a single Trp in a homogeneous environment. In addition, a minor Gaussian, centered at ~305 nm, indicated a slight contribution, to the whole fluorescence, of the two Tyr residues (Y1236 and Y1243). In the presence of DM or DPC, and for both peptides, the spectral decomposition yielded two well separated components for Trp fluorescence (Fig. 2A and 2B). For TM17, the low-polarity component (at 314–319 nm) and the higher polarity component (at 347–349 nm) were about equally weighted. For mTM17, both components were slightly red-shifted and the lower polarity component was dominant. Small differences were also observed as a function of the detergent used. These data indicate that, in the bound peptide, Trp may experience exposure to environments of various polarities. In addition, Tyr contribution was slightly quenched in solvents as compared to detergent micelles. This suggests that Tyr–Trp (intramolecular) Förster resonance energy transfer occurs in these solvents to a higher extent than for detergent-bound peptides.

3.2. Steady-state fluorescence spectra of model peptides P3 to P13 in DPC

For reference, we recorded the emission spectra in DPC of all the single tryptophan-containing Pn model peptides (P3 to P13), as previously done in DM [17]. In DM, Trp was found to be located at various depths in the micelle, from the polar

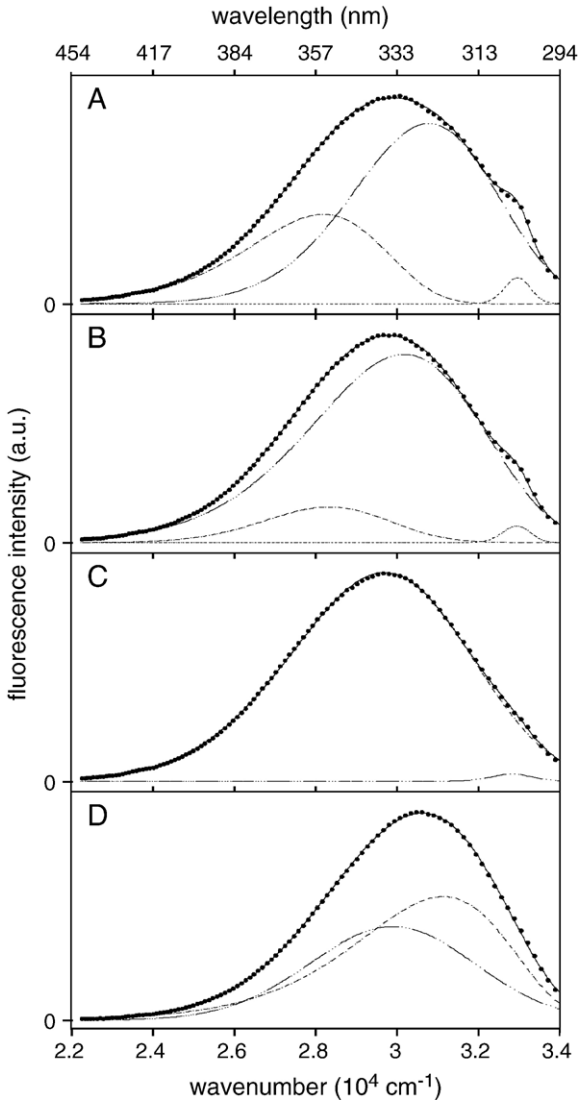

Fig. 2. Decomposition of mTM17 steady-state fluorescence spectra in various media into log-normal Gaussian components. Comparison with the model peptide P7 in DPC. mTM17 in DM (A), DPC (B) and methanol (C); P7 in DPC (D). Normalized raw spectra (closed circles) are from Figs. 1 and 3, presented with a wavenumber scale (lower scale). (Dashed lines), elementary Gaussian components, obtained as described in Materials and methods; (continuous line), spectra reconstituted from their components.

headgroup region, to the center of the micelle core depending on its position in the model peptide. The normalized spectra in DPC (Fig. 3) clearly illustrate the shift of the raw spectrum and of the resulting λ_{max} in response to Trp location in the micelle. The λ_{max} values (Table 2) were very similar for P3, P5 and P7 (329 nm), and then decreased from P7 to P13. This variation with Trp position is similar to that previously observed in DM [17] (as also reported in Table 2), except that the λ_{max} value was slightly higher in the plateau region in DPC, indicating a slightly higher polarity.

We also analyzed the steady-state fluorescence spectra of the Pn model peptides in DPC by log-normal Gaussian decomposition (Fig. 2D, for P7 as an example and Table 2). Here again, two components, with λ_{max} corresponding to intermediate (320–340 nm) and low (310–321 nm) polarity, accounted

Table 1
The parameters of the log-normal Gaussian components of the steady-state fluorescence emission spectra of TM17 and mTM17 in detergent micelles and pure solvents

Sample	log-normal Gaussian #1			log-normal Gaussian #2			log-normal Gaussian #3		
	λ_{max} (nm)	FWHM (cm^{-1})	Spectrum peak height (%)	λ_{max} (nm)	FWHM (cm^{-1})	Spectrum peak height (%)	λ_{max} (nm)	FWHM (cm^{-1})	Spectrum peak height (%)
TM17 in DPC	347	3862	44	314	3293	47	302	754	9
TM17 in DM	349	3897	43	319	3396	49	303	745	8
TM17 in DMSO	339	4953	94	–	–	–	305	2127	6
mTM17 in DPC	351	3817	18	331	5042	76	303	814	6
mTM17 in DM	354	4057	33	324	4158	59	303	761	8
mTM17 in MetOH	337	5214	97	–	–	–	304	1238	3

The decomposition procedure is detailed in Materials and methods. λ_{max} is calculated as $1/\nu_m \times 10^4$ and the spectrum peak height as $I_{mi}/\Sigma I_{mi}$. FWHM is the full width at half maximum.

for Trp fluorescence. These components had similar weighting and widths (except for P13). The major change from P3 to P13 is a significant blue-shift (by 10 to 20 nm) for both components. The previously studied raw spectra of Pn in DM were analyzed similarly: similar trends were observed but the lower wavelength component was blue-shifted by a few nm (to 304–314 nm) with respect to that in DPC and the components were significantly narrower.

The most straightforward interpretation of these data is that occurrence of transverse diffusion of the model peptides around a mean location in the mixed peptide-detergent micelles accounts for this apparent heterogeneity.

3.3. Steady-state fluorescence quenching of TM17 and mTM17 by brominated detergents

We have previously shown, using the set of Pn model peptides, that Trp quenching in DM micelles by its brominated analogs (BrDM and BrUM) was dependent upon Trp depth in the micelle [17]. Quenching by these dibrominated analogs of DM was highly efficient so that ~95% quenching was

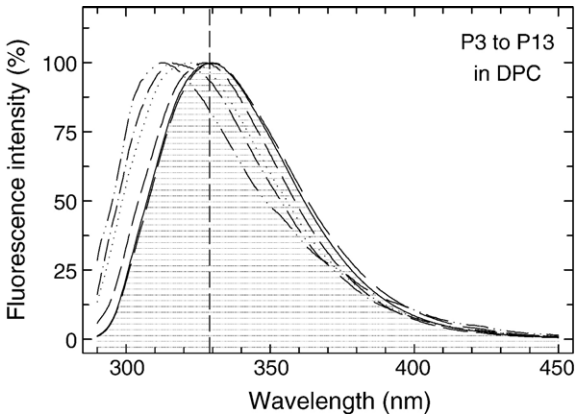

Fig. 3. Fluorescence emission spectra of the Pn model peptides in DPC micelles. Normalized emission spectra of P3 (solid line and hatched area), P5 (medium dashed line), P7 (short dashed line), P9 (dotted line), P11 (dashed-dotted line) and P13 (dashed-double dotted line), (8 μM) in 10 mM potassium phosphate buffer, pH 7.5, supplemented with 4 mM DPC, at 20 °C. λ_{ex} was set at 278 nm. Slit widths were 1.25 mm (bandwidths ~ 5 nm) for both excitation and emission. Spectra were recorded after a short period of equilibration (2–3 min). The vertical dashed line indicates λ_{max} for P3.

experimentally determined for these model peptides as well as for TOE [21] and for fragments of PMP1 [41], a single span membrane protein, when solubilized in pure brominated detergent micelles.

Fig. 4A shows the fluorescence quenching curves of TM17 and mTM17 in mixed micelles of DM with BrDM, plotted as a function of BrDM molar ratio. The curves were fitted as previously described (see legend to Fig. 4), yielding two parameters: the lattice parameter n, characteristic of the curvature, and the residual fluorescence of the peptide in the presence of pure brominated detergent micelles (i.e. at X (BrDM) =1), F_{min}/F_0. The inset shows the calibration graph of n previously obtained with the whole set of Pn model peptides and the horizontal lines corresponding to the n values for TM17 and mTM17. Panel B shows the results of similar experiments with BrUM rather than BrDM.

Both TM17 and mTM17 were significantly quenched in pure BrDM micelles (panel A), as shown by the low residual fluorescence F_{min}/F_0 (~20%), an unambiguous indication that a major fraction of the Trp in these peptides was in close contact with the detergent acyl chain. However, this level of residual fluorescence is higher than the values obtained for the model peptides (F_{min}/F_0~ 5%). The shape of the curve is determined by the parameter n. The n values obtained with BrDM reflect the accessibility of Trp to the middle of the detergent acyl chain—the C7 to C8 carbons to which the two bromine atoms are bound. The calibration curve of n in BrDM (inset) shows that n is a complex function of Trp position in the micelle. The quenching curve for mTM17 is positioned slightly higher on the axes than that for TM17, and the values obtained with mTM17 and TM17 (n=2.0 and 2.2, respectively) are slightly or significantly below those of the calibration curve, indicating lower Trp accessibility for these two peptides than for the model peptides.

Similar trends were observed in BrUM (Fig. 4B). With this detergent, we tested the accessibility of Trp to the end of the detergent acyl chain (C10 and C11 carbons), to which the two bromine atoms are bound. F_{min}/F_0 values were higher (20–28%) for mTM17 and TM17 than for the model peptides (~ 8% as a mean in this detergent). The n values for mTM17 and TM17 (respectively 2.9 and 3.2) were significantly higher than those in BrDM – as reported for the model peptides – but the values obtained were significantly lower than the values obtained for any of the model peptides (inset to panel B).

Table 2
Parameters of the log-normal Gaussian components of the steady-state fluorescence emission spectra of model peptides P3 to P13 in DPC and DM

Sample	Raw spectrum	log-normal Gaussian #1			log-normal Gaussian #2		
	λ_{max} (nm)	λ_{max} (nm)	FWHM (cm^{-1})	Spectrum peak height (%)	$\lambda_{max\ (nm)}$	FWHM (cm^{-1})	Spectrum peak height (%)
P3 in DPC	329	339	4501	49	320	4005	51
P5 in DPC	330	340	4639	47	321	4108	53
P7 in DPC	328	334	4760	43	321	4541	57
P9 in DPC	322	334	4562	46	310	3845	54
P11 in DPC	316	328	5071	48	310	4377	52
P13 in DPC	314	320	7618	43	311	3963	57
P3 in DM	327[a]	339	3666	50	314	2765	50
P5 in DM	326	336	4216	61	311	2931	39
P7 in DM	327	335	3916	59	311	2667	41
P9 in DM	321	328	4056	59	304	2898	41
P11 in DM	317	328	4034	58	304	2615	42
P13 in DM	313	327	3854	54	304	2379	46

The decomposition procedure is detailed in Materials and methods. λ_{max} is calculated as $1/\nu_m \times 10^4$ and the spectrum peak height as $I_{mi}/\Sigma I_{mi}$. FWHM is the full width at half maximum.
[a] λ_{max} for Pn in DM are from [17].

These data indicate that both TM17 and mTM17 interact with micelles, but also show that they are not inserted into these micelles in the same way as the model peptides: a slightly higher proportion of Trp is out of reach of bromine atoms and the cooperativity for quenching is lower. In addition, the Trp in mTM17 appears to be slightly less accessible to detergent acyl chains than that in TM17. A plausible explanation for these data, in agreement with emission spectral data, is that Trp may be located closer to the surface of the micelle for TM17 and mTM17 than for any of the model peptides, possibly due to an interfacial location of the fragments in the micelle. However, at this step, we cannot exclude the fact that the presence of some oligomers may also contribute to Trp shielding from bromine atoms.

3.4. Acrylamide quenching of TM17 and mTM17 in DM and DPC micelles. Comparison with model peptides

If Trp in TM17 or mTM17 was less accessible to detergent chains than in model peptides, it can be expected to be more accessible to water-soluble quenchers. We therefore assessed its accessibility to acrylamide, a neutral, water-soluble quenching probe. Acrylamide was chosen in preference to iodide to avoid the specific charge effects previously shown to occur with DPC [32].

The Stern–Volmer plots of fluorescence quenching obtained for TM17 and mTM17 in the presence of DM or DPC micelles are shown in Fig. 5. For both peptides, linear fits were adequate, typical of a simple collisional (dynamic) mechanism. The apparent accessibility to acrylamide (Fig. 5 and K_{sv} in Table 3) was one half to one quarter that of NATA in buffer, taken as a reference. A comparison of the bimolecular quenching constants k_q (see Table 3) indicated similarly restricted accessibility (of ~35%) of TM17 to acrylamide in both DM and DPC, whereas mTM17 appeared to be more accessible in both detergents (~65%).

For comparison, representative Stern–Volmer plots of quenching for Pn model peptides in DPC micelles are shown in Fig. 6. The apparent accessibility of Trp to acrylamide decreases from P3 to P13, reaching very small values. Quenching parameters are given in Table 3 and accessibilities with respect to NATA ranged from 34 to 13%, consistent with Trp being located in the hydrophobic core of the micelle, at various distances from the center.

Trp in TM17 or mTM17 appears to be more accessible to acrylamide than in any of the model peptides. This observation again highlights the particular properties of both MRP1 fragments.

The fraction of fluorescence quenched by acrylamide exceeded the fraction not quenched by brominated detergents (F_{min}/F_0). This suggests that some Trp may be accessible to both acrylamide and brominated detergent chains. We assessed the extent to which quenching by acrylamide and quenching by brominated detergents were complementary, by measuring quenching by 0.2 M (final concentration) acrylamide for TM17 and mTM17, in the presence of pure brominated detergent, BrDM or BrUM, in the experimental conditions used for the Stern–Volmer plots (λ_{exc}=295 nm). In these conditions, the quenching by pure brominated detergent (4 mM in buffer) of the Trp in TM17 and mTM17 was similar to that for excitation at 280 nm, resulting in 18 to 28% residual fluorescence with respect to peptide in DM. In all cases, the residual fluorescence was further reduced to 10 to 12% in the presence of brominated detergent and 0. 2 M acrylamide. Thus, Trp can be quenched by acrylamide or brominated detergent, and in some cases, by both. These data seems to discard the possibility of significant oligomerization of the peptides.

3.5. Time-resolved fluorescence intensity measurements for MRP1 fragments in solvents, DM and DPC

Trp fluorescence lifetime distributions are sensitive indicators of ground state heterogeneity (such as conformer distribution [43–47]) and reactions implying the excited-state (energy transfers, dipolar relaxation [48]).

In neat solvents (DMSO for both peptides and MeOH for mTM17), the analysis of the fluorescence decays showed one major population with a long lifetime indicating one major

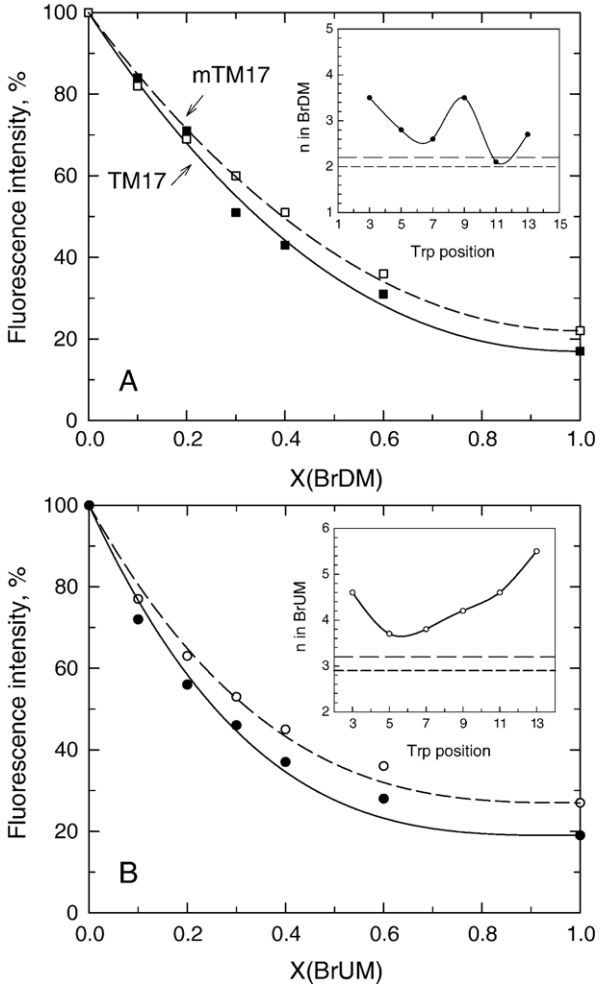

Fig. 4. Quenching curves of TM17 and mTM17 fluorescence in mixed micelles of BrDM/DM or BrUM/DM. (A) TM17 (closed symbols) or mTM17 (open symbols) (5 μM) was added to 10 mM potassium phosphate buffer pH 7.5 supplemented with a mixture of BrDM and DM, at a final total detergent concentration of 4 mM, at 20 °C. The resulting fluorescence intensity was recorded for 200 s, to allow similar equilibration, and the final fluorescence intensity was corrected for the blank value (detergents in buffer) and plotted as a function of the molar fraction of brominated detergent X, defined as X=[BrDM]/([BrDM]+[DM]). X was varied between 0 (pure DM micelles) and 1 (pure BrDM micelles). λ_{ex} was set at 280 nm and λ_{em} at 335 nm, with slit widths of 1.25 mm for both excitation and emission. Data points are the means of duplicate measurements. The function $F/F_0=(1-F_{min}/F_0)(1-X)^n+F_{min}/F_0$ was fitted to the data (see Materials and methods). The inset shows the calibration curve of n for BrDM obtained with six Pn model peptides (continuous line, closed symbols), where n is plotted as a function of Trp position in the peptide [17]. The two horizontal lines represent the n values obtained here for TM17 (long dash) and mTM17 (short dash). (B) As above, but with BrUM instead of BrDM. Here, each data point is the mean for two independent experiments. Inset: n values are also shown on the calibration plot for BrUM obtained with the Pn model peptides (continuous line, open symbols).

conformation of the Trp side-chain (Fig. 7A). The high dielectric constant of DMSO favors one Trp ground-state conformer [49] whereas the whole peptide is likely unfolded [50]. MeOH also favors one conformer with a similar lifetime as in DMSO but in a α-helical global structure. In contrast, in detergent micelles, lifetime distributions are more complex for both peptides. We observed three principal lifetime populations for TM17 in DPC (Fig. 7B) and four in DM (Table 4). mTM17

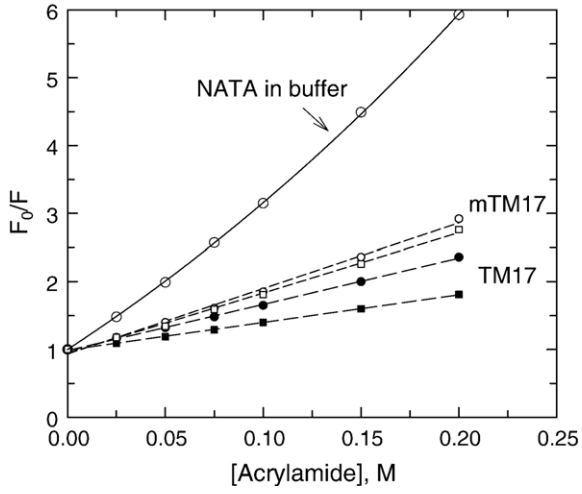

Fig. 5. Stern–Volmer plots of acrylamide quenching of TM17 and mTM17 in DPC and DM micelles. 8 μM TM17 (closed symbols) or mTM17 (open symbols) was added to 10 mM phosphate buffer pH 7.5, at 20 °C, supplemented with 4 mM DPC (circles) or DM (squares). Aliquots of acrylamide were then added sequentially, at 100 s intervals. Fluorescence intensity was continuously recorded with λ_{ex} set at 295 nm and λ_{em} set at 340 nm. Bandwidths were 1.25 mm for excitation and 2.5 mm for emission. The fluorescence intensities obtained at each acrylamide concentration were corrected for blank values. For comparison, a similar experiment was also performed with NATA (5 μM) in buffer (open circles) (λ_{em}=354 nm in this case). A straight line was fitted to the data for both peptides in the presence of detergent, whereas the modified Stern–Volmer equation was used for NATA.

showed also four lifetime populations in DM. This indicates a more heterogeneous conformer distribution in micelles as compared to the solvents. The similarity of the lifetime distribution profiles for mTM17 and TM17 in DM micelles shows that the presence of the N-terminal charged residue (K) has little effect on the Trp conformer distribution and their close environment, at least in this detergent.

3.6. Time-resolved fluorescence anisotropy measurements of MRP1 fragments in solvents, DM and DPC

Anisotropy measurements were performed in order to characterize the rotational dynamics of the systems under

Table 3
Parameters of TM17, mTM17 and of transmembrane model peptides Pn fluorescence quenching by acrylamide

Sample	Medium	<τ> (ns)	K_{sv} (M^{-1})	k_q (M^{-1} s^{-1}) (% of reference)
NATA	Buffer	3.0	17.5	5.8×10^9 (100%)
TM17	DM micelles	2.1	4.07	1.9×10^9 (33%)
TM17	DPC micelles	2.9	6.79	2.3×10^9 (39%)
mTM17	DM micelles	2.0	8.86	4.4×10^9 (75%)
mTM17	DPC micelles	2.9	9.63	3.3×10^9 (57%)
P3	DPC micelles	4.6	6.86	1.5×10^9 (26%)
P7	DPC micelles	3.0	5.81	2.0×10^9 (34%)
P9	DPC micelles	2.7	3.75	1.4×10^9 (24%)
P13	DPC micelles	2.9	2.14	0.74×10^9 (13%)

The mean lifetime was $<\tau>=\Sigma\alpha_i\tau_i$. For NATA, the mean lifetime was taken from [89]. For peptides,<τ>values were taken from Table 4, except for mTM17 (the value of TM17 in DPC was taken). K_{sv} were the slopes from Figs. 5 and 6. $k_q=K_{sv}/<\tau>$.

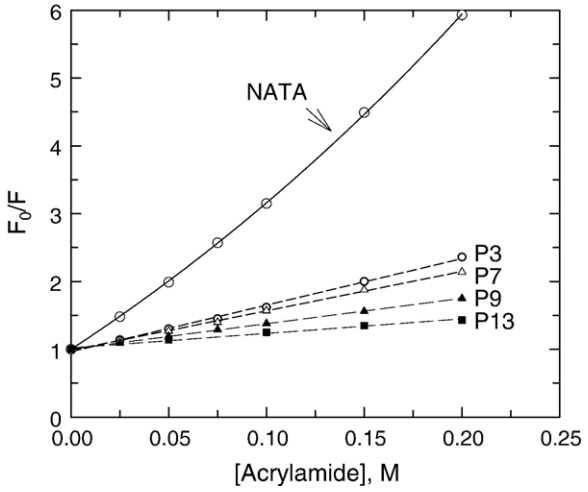

Fig. 6. Representative Stern–Volmer plots of acrylamide quenching of Pn model peptides in DPC micelles. Pn model peptides (5 μM) were added to 10 mM phosphate buffer pH 7.5, supplemented with 4 mM DPC, at 20 °C. Aliquots of acrylamide were then added sequentially, at 100 s intervals. Fluorescence intensity was continuously recorded with λ_{ex} set at 295 nm and λ_{em} at 340 nm for P3 and P7 and 320 nm for P9 and P13 (slightly above and below their λ_{max} values, respectively, to avoid the Raman peak maximum close to 330 nm in these conditions). Bandwidths were 1.25 mm for excitation and 2.5 mm for emission. The fluorescence intensities obtained at each acrylamide concentration were corrected for blank values. The plot for NATA in buffer alone is shown for comparison (open circles). A straight line was fitted to the data for the peptides in the presence of DPC.

study. The parameters of the rotational correlation time distributions, obtained from MEM analysis of polarized fluorescence decays, are shown in Table 5. In neat solvents, we observed for both peptides a single rotational correlation time (θ_3) in the nanosecond range representing their Brownian motions. Its values for both peptides are consistent with a monomer in DMSO or a dimer in MeOH, taking into account the viscosity of the solvents ($\eta_{20°C}$=2.1 cP and 0.6 cP for DMSO and MeOH respectively). Subnanosecond rotational correlation times are also observed (Table 5), describing the fast local motion of the Trp side-chain around the C_α–C_β–C_γ bonds. Using the wobbling-in-cone model for this motion [51], we estimated the cone semi-angle ω_{max} to be 45–50°.

In DM and DPC micelles, the values of the Brownian rotational correlation times are increased by about one order of magnitude with respect to that in neat solvents, reflecting the incorporation of the peptides into detergent micelles (Table 5). In DM, the mixed peptide–detergent micelles have approximately the same rotational correlation time (and therefore the same size) than pure DM micelles (theoretical value: 21 ns, without taking into account micelle hydration, see Materials and methods). In DPC, the mixed micelles could be larger than pure DPC micelles (theoretical value of 7.4 ns). In both detergents, a second nanosecond rotational correlation time, 10–20 times shorter than that for Brownian dynamics, describes the local motions of Trp and/or the segmental motion of TM17, which becomes strongly slowed down as compared to the neat solvent. This component displayed a larger contribution to the anisotropy in DPC than in DM (as seen from the β_2 values), suggesting a larger local flexibility of the peptide in the former than in the latter detergent. A third subnanosecond component of small amplitude is detected in DPC and is likely present in DM since the initial anisotropy value $A_{t=0}$ is smaller than the intrinsic anisotropy A_0 of Trp [52] measured in glass medium. The wobbling-in-cone motion – which takes into account all subnanosecond motions, even those not resolved in the decay – was significantly more restricted in both detergents than in the solvents, as shown by the (ω_{max}) values obtained (Table 5). In DM, mTM17 displays a wobbling-in-cone motion of larger amplitude than that for TM17.

3.7. Time-resolved fluorescence intensity measurements of model peptides P3 to P13 in DPC

The time-resolved fluorescence parameters of the single-Trp containing Pn model peptides previously measured in DM [17], were also analyzed in DPC, to provide a reference for transmembrane peptides incorporated in these micelles. The results are shown in Table 6. For all Pn peptides, fluorescence intensity decays were represented by three lifetime populations. The main trend in variation from P3 to P11 (P13 behaved in an unusual manner) was a significant decrease in the relative am-

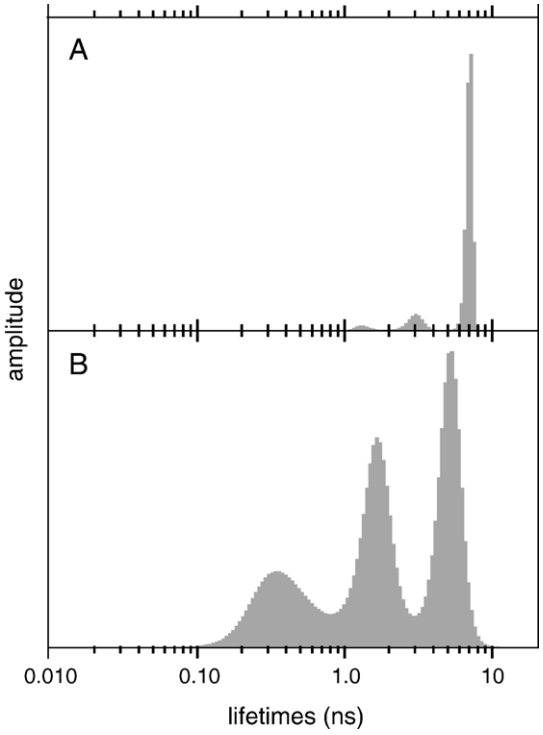

Fig. 7. MEM recovered lifetime distributions of TM17 in DMSO or DPC micelles. (A) TM17 was used at a concentration of 10 μM in DMSO. λ_{ex}= 295 nm, λ_{em}=338 nm, excitation and emission bandwidths: 4 and 8 nm, respectively. The normalized area α_i and barycenters τ_i of each peak of the lifetime distribution were as follows: α_1=0.01, α_2=0.13, α_3=0.86; τ_1=0.33 ns, τ_2=2. 5 ns, τ_3=6. 9 ns; χ^2=1.03. (B) TM17 was used at a concentration of 5 μM in 10 mM phosphate buffer (pH 7.5) containing 4 mM DPC. λ_{ex}=292 nm, λ_{em}=332 nm, bandwidths as above. α_1=0.23, α_2=0.38, α_3=0.38; τ_1=0.48 ns, τ_2=1. 7 ns, τ_3=5. 4 ns. χ^2=1.05. The temperature was constant at 20 °C in all cases.

Table 4
Parameters of the fluorescence intensity decays of TM17 and mTM17 in various media

Peptide	Solvent	α_1	α_2	α_3	α_4	τ_1 (ns)	τ_2 (ns)	τ_3 (ns)	τ_4 (ns)	$<\tau>$ (ns)	χ^2
TM17	DMSO	0.01		0.13	0.86	0.33		2.5	6.9	6.3	1.03
	DM	0.27	0.33	0.28	0.12	0.3	1.2	3.0	6.8	2.1	
	micelles	(±0.07)	(±0.04)	(±0.03)	(±0.07)	(±0.1)	(±0.2)	(±0.7)	(±1.3)	(±0.2)	
	DPC	0.22		0.37	0.41	0.4		1.6	5.3	2.9	
	Micelles	(±0.05)		(±0.02)	(±0.07)	(±0.2)		(±0.4)	(±0.3)	(±0.2)	
mTM17	DMSO			0.13	0.87			3.0	7.0	6.5	1.06
	Methanol			0.20	0.80			1.6	4.9	4.3	1.08
	DM	0.21	0.44	0.20	0.17	0.13	1.2	3.2	6.4	2.0	
	Micelles	(±0.02)	(±0.08)	(±0.02)	(±0.04)	(±0.02)	(±0.1)	(±0.2)	(±0.2)	(±0.3)	

Experimental conditions were as for Fig. 7 for TM17. A different experimental setup was used for the experiments with mTM17: the source was a LED (light-emitting diode) with maximal emission at 298 nm. mTM17 was used at a concentration of 30 μM in methanol and in DMSO, with λ_{ex}=295 nm, λ_{em}=337 nm, 16 nm slits for both excitation and emission and a cutoff filter (T50% at 306 nm) on the emission pathway. In DM, mTM17 was used at a concentration of 15 μM. α_i is the normalized area and τ_i the barycenter of each peak i of the lifetime distribution obtained in MEM analysis. The mean lifetime $<\tau>$ is calculated as $<\tau>=\Sigma\alpha_i\tau_i$. Either representative data (with χ^2 values) or mean values (±standard error) over 2–3 experiments are given.

plitude of the longer component α_3, and a decrease in the two nanosecond lifetimes (τ_2 and τ_3). As a result, the mean lifetime $<\tau>$ halved between P3 and P11 like in DM [17]. Higher $<\tau>$ values than in DM (up to 30% for P9) were however observed in DPC (in DM, the distribution also displayed a minor contribution of a fourth, very short component). These higher $<\tau>$ values mainly result from a higher contribution of the longest lifetime population (i.e. α_3) in DPC than in DM. They likely reflect differences in the local conformer equilibrium of the Trp residue [45,53] under the influence of the different polar headgroups of the detergent (sugar and choline for DM and DPC, respectively) on the packing and/or dynamics of the whole micelle.

3.8. Time-resolved fluorescence anisotropy measurements for model peptides P3 to P13 in DPC

Table 7 shows the parameters of the anisotropy decays of Trp in the model peptides in interaction with DPC micelles. The rotational correlation time distribution showed subnanosecond and nanosecond rotational motions. The mean value of the major long rotational correlation time over the six peptides was in the range of 17 ns (±6 ns). This is significantly shorter than the mean value previously obtained for Pn-DM mixed micelles (36±5 ns), consistent with a smaller size of the Pn-DPC mixed micelles. The shorter components reflect the local mobility of Trp with respect to the micelle. The local subnanosecond motion was characterized by a mean "wobbling-in-cone" angle close to 32° (±4°)—similar to that previously measured in DM (30° ± 3°). The value of the rotational angle increased from P3 to P13 by 30% (Table 7), suggesting that the local constraints to the Trp rotation are stronger near the water/micelle interface than in the center of the DPC micelle.

3.9. CD spectra of mTM17 in various media

The secondary structure of mTM17 was assessed by circular dichroism (Fig. 8A). In all conditions, the four successive scans registered for each spectrum were superimposable. The spectrum for mTM17 in methanol, as a reference, had an overall shape characteristic of an α-helix signal, with a strong positive maximum at 191 to 192 nm and two negative minima at 208 and ~220 nm. The α-helix content was estimated at 77% from the value of $[\theta]_{222nm}$ [38]. Note that the $[\theta]_{191}/[\theta]_{208}$ ratio,

Table 5
Parameters of the fluorescence anisotropy decays of MRP1 fragments in various media

Peptide	Solvent	β_1	β_2	β_3	θ_1 (ns)	θ_2 (ns)	θ_3 (ns)	$A_{t=0}$	ω_{max} (°)	χ^2
TM17	DMSO[c]	0.127	0.009	0.092	0.34	0.55	2.9	0.228	45	1.09
	DM[b]		0.016	0.123		1.4	28	0.139	17	
	micelles		(±0.006)	(±0.012)		(±0.5)	(±5)	(±0.013)	(±3)	
	DPC[b]	0.016	0.042	0.096	0.50	2.4	22	0.154	17	
	micelles	(±0.019)	(±0.011)	(±0.004)	(±0.04)	(±0.6)	(±3)	(±0.011)	(±9)	
mTM17	Methanol[a]		0.158	0.071		0.14	1.5	0.229	50	1.07
	DMSO[a]		0.113	0.069		0.21	2.0	0.182	50	1.03
	DM[a]			0.133			16	0.133	37	
	Micelles			(±0.023)			(±1)	(±0.023)	(±5)	

Experimental conditions were as described in Table 4. The anisotropy β_i is the area and the rotational correlation time θ_i is the barycenter of peak i of the rotational correlation time distribution. $A_{t=0}$ is the anisotropy at time zero, with $A_{t=0}=\Sigma\beta_i$. The semi-angle ω_{max} of the wobbling-in-cone subnanosecond motion was calculated from: $\Sigma\beta_{ns}/A_0=[1/2\cos\omega_{max}(1+\cos\omega_{max})]^2$, which gives: $\omega_{max}=\mathrm{Arccos}1/2[(1+8(\Sigma\beta_{ns}/A_0)^{1/2})^{1/2}-1]$, where A_0 is Trp anisotropy in the absence of depolarization and β_{ns} the anisotropies of the nanosecond components. Values of 0.251, 0.240 and 0.154 were taken for excitation with the PLS295[(a)] and with the synchrotron at 292[(b)] or 295[(c)] nm, respectively. The A_0 value of 0.251 was calculated from the wavelength convolution of the nanoLED optical power emission with the intrinsic anisotropy of NATA (from [52]). Representative data (with χ^2 values) or mean values (± s.d.) are given.

Table 6
Parameters of the fluorescence intensity decays of model peptides P3 to P13 in DPC micelles

Peptide	Solvent	α_1	α_2	α_3	τ_1 (ns)	τ_2 (ns)	τ_3 (ns)	$<\tau>$ (ns)	χ^2
P3	DPC	0.11	0.18	0.71	0.6	2.9	5.7	4.6	1.07
P5	–	0.16	0.26	0.58	0.7	2.7	5.9	4.3	1.03
P7	–	0.23	0.34	0.43	0.6	2.3	4.8	3.0	1.03
P9	–	0.28	0.41	0.31	0.6	2.1	5.3	2.7	1.05
P11	–	0.38	0.25	0.37	0.5	2.2	4.6	2.3	1.03
P13	–	0.13	0.23	0.64	0.3	0.9	4.1	2.9	1.15

Pn peptides were used at a concentration of 10 μM in 25 mM potassium phosphate buffer pH 7.5 supplemented with 4 mM DPC, at 20 °C. λ_{ex}=280 nm λ_{em}=327 nm (for P3, P5, P7), 321 nm (for P9), 316 nm (for P11) and 312 nm (for P13), as in our previous experiments in DM.

which is independent of concentration measurements, is also characteristic of an α-helix. Absolute ellipticities were comparatively low for mTM17 in buffer, with significant differences in the shape of the spectrum (a weak positive peak at ~190 nm and a single minimum at ~215–217 nm). DPC had a strong helix-promoting effect on this peptide, as compared to buffer alone, resulting in an α-helix content of about 50%, as calculated from $[\theta]_{222nm}$. DM had the same overall effect but with a slightly less efficiency than DPC.

We made this analysis more specific, with the aim of identifying the other secondary structure components, by deconvoluting the CD spectra with two programs and the same two sets of reference proteins with each program, which should improve the reliability of predicted structures [39,40]. The fractions of α-helix, β-sheets, turns and unordered structures are presented as histograms in Fig. 8B. The four analyses gave consistent results so that the contribution of the main structural elements could be reliably estimated. In detergent, the main fraction of α-helix accounted for about 45% of the peptide, with unordered structures accounting for about 25% of the peptide. In buffer, β-strands made a significant contribution to secondary structure.

As the N-terminal mutation is unlikely to change the structural propensity of the peptide, and the lack of a charged residue may result in the N-terminus being inserted more deeply into the micelles, TM17 would be expected to contain at least as much α-helix in micelles. However, as DMSO absorbs strongly in the spectral region used for CD experiments, we could not monitor TM17 spectra in similar conditions.

Table 7
Parameters of the fluorescence anisotropy decays of model peptides P3 to P13 in DPC micelles

Peptide	β_1	β_2	β_3	θ_1 (ns)	θ_2 (ns)	θ_3 (ns)	$A_{t=0}$	ω_{max} (°)	χ^2
P3	–	0.020	0.103	–	1.1	14	0.123	27	1.02
P5	0.017	0.038	0.079	0.6	3.0	17	0.134	29	1.00
P7	–	0.033	0.094	–	1.4	14	0.127	26	0.97
P9	0.029	0.039	0.060	0.4	4.1	15	0.128	34	1.02
P11	0.068	0.026	0.063	0.1	1.7	12	0.143	37	1.02
P13	0.010	0.018	0.063	0.5	2.0	30	0.126	39	1.01

Conditions were as in Table 6. The excitation wavelength was 280 nm; A_0 was therefore taken as 0.173 [52].

3.10. Steady-state fluorescence spectra of TM17 and mTM17 in phospholipid vesicles

The behavior of each peptide in the presence of membrane vesicles was studied for the sake of comparison with the micellar systems. Steady-state fluorescence spectra were performed on two types of samples. They were prepared either by addition of the peptide (5 μM) to a dispersion of sonicated membrane vesicles (egg PC alone or a egg PC/PS 1/1 (mol/mol) mixture, lipid/peptide molar ratio of ~ 100) or co-evaporation of a chloroformic solution of peptide and phospholipids and dispersion in buffer by sonication. The fluorescence emission intensity of each peptide in the absence of lipid vesicles was maximum at ~ 335–336 nm and decreased as a function of time, indicating a time-dependent auto-association. In the presence of either PC or PC/PS vesicles, the maximum slightly shifted to 331–332 nm in both types of preparations (not shown), close to the values in detergent micelles.

4. Discussion

This study focused on the interaction with membrane mimics of TM17, a functionally important predicted TM fragment of

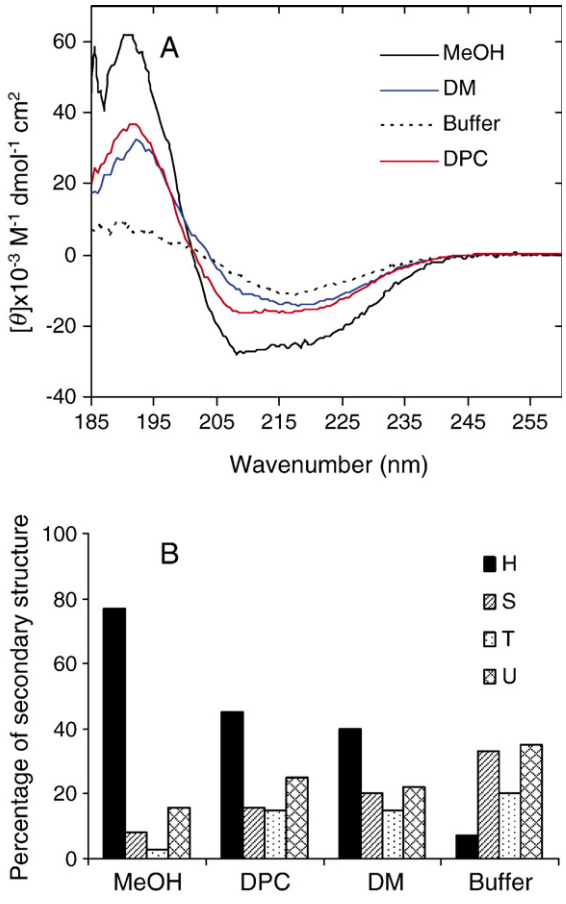

Fig. 8. Far UV CD spectra of mTM17 in various media. (A) Data are represented as molar ellipticity per residue. Spectra were registered with 100 μM mTM17 in methanol (continuous black line) or 25 μM mTM17 in buffer alone (dashed line) or in the presence of 4 mM DPC (red line) or DM (blue line). Further details are provided in Materials and methods. (B) Histograms for the various structural elements (H: helix, S: β-strands, T: turns, U: unordered structures).

MRP1 (ABCC1) in the current consensus topological model [54]. This model was not straightforward to establish since various plausible predictions have been successively proposed. It takes into account, in addition to classical hydropathy analysis, experimental determination of extra-cellular N-glycosylation sites, the orientation of various loops by epitope insertion and immunofluorescence, as well as comparison with similar proteins. In the absence of 3-D structure, validation of the model is not yet possible. MRP1 is rich in Trp residues, with 30 in total, 12 of which are located within or very close to predicted TM segments. Trp is heterogeneously distributed among these TM segments, which may have between zero (e.g. TM11 to TM15) and three Trp (TM2) residues. This distribution is probably not purely fortuitous. Due to their specific properties, including H-bonding ability, and cation-π effects [55,56], membrane protein Trp were shown to be preferentially located at interfacial regions of the membrane (e.g. [57]) where they may have several functions, including TM anchorage in the membrane, protein stabilization and substrate binding. TM17 contains a single Trp (W1246) residue, making it possible to use this fragment to investigate the local structure, dynamics and location of the peptide in membrane mimics by fluorescence spectroscopy. W1246 is thought to be involved in substrate binding and the substrate translocation pathway [2,11]. Its position in the sequence, close to the cytoplasmic C-terminus of TM17, also suggests a possible role in anchoring TM17 in the membrane. We studied a synthetic TM17 fragment encompassing the predicted TM17 fragment and slightly extended at the C-term, so as to include the functionally important Arg_{1249}. We studied in addition a synthetic mutant, mTM17, bearing an additional positive charge in the N-term. Peptide secondary structure elements were also characterized under the same conditions by CD spectroscopy.

As previously described , we used DM and DPC micelles as membrane mimics. DM is one of the most suitable detergents for the solubilization, purification and stabilization of activity of a wide range of membrane proteins including MRP1 (see [58–60] for comparative studies with numerous detergents; [15,61–63] for recent purifications of overexpressed proteins). DM has also been used to crystallize some of the few membrane proteins for which X-ray structures have been resolved [64,65]. We previously made synthesize brominated analogs of this detergent for topological studies by fluorescence spectroscopy [20,21], which were used in the present work. These detergents could also be visualized by X-ray diffraction in membrane protein crystals, due to their high electron density ([66–68] and ref. therein). DPC is the detergent of choice in NMR experiments, as its micelles are small, like those of SDS, but, beyond this technical reason which is not so stringent for fluorescence, above all DPC very efficiently reproduces the interfacial region of phospholipid bilayers with water, with a similar head group as phosphatidylcholine [25]. It is used more specifically for structural studies of amphiphilic peptides [69–72], membrane protein fragments [73,74] and small proteins (e.g. [75]).

TM17 and mTM17, studied at micromolar concentrations sufficient for fluorescence and CD experiments, were both readily solubilized in the presence of excess detergent micelles. This is shown for instance by the strong fluorescence quenching (up to ~ 80%) of these fragments in mixed micelles of DM and one of its brominated analog, BrDM or BrUM, because this quenching requires close contact between Trp and the bromine atoms, located on the detergent acyl chain. In addition, the significant accessibility of Trp to acrylamide seems to rule out the presence of oligomers, since no Trp seems to be shielded from both quenchers. Further evidence is provided (i) by the structuring effect of the detergent, (ii) by rotational correlation time measurements – which reflect the whole peptide–detergent complex rotation – and (iii) by the more stable fluorescence intensity than observed for peptide in buffer alone.

The maximum wavelength of Trp fluorescence emission, λ_{max}, is very sensitive to the polarity – or local electric field – of the Trp environment (e.g. [76] and ref. therein), with red-shifts observed as polarity increases. In proteins, λ_{max} may vary from 308 nm (for a completely buried Trp residue) to 355 nm (for a Trp residue fully exposed to water) [34]. Using Pn transmembrane model peptides in DM [17] or DPC (present study) micelles, we have shown that the λ_{max} of the raw spectra for Pn ranges from 314 nm, for a Trp residue located in the core of the micelle, to 327–330 nm, for a Trp residue located close to the polar headgroup region. In the present study, each of these spectra was further decomposed into two log-normal Gaussian components, for which λ_{max} ranged from 304 to 340 nm, reflecting the wide range of polarity (or local electric field) experienced by Trp residues within these micelles. This data analysis indicated significant fluctuations in peptide positions, without significant contact between Trp and the bulk solvent. These results are consistent with molecular dynamics simulations, indicating fast dynamics, in the nanosecond time range, of detergent molecules in DPC micelles [77,78] and bound peptides in mixed micelles [79].

The raw emission spectra of the MRP1 fragments, TM17 and mTM17, interacting with detergent micelles, were characterized by a λ_{max} at 332–335 nm, corresponding to a Trp environment more polar than that experienced by the Pn model peptides. The analysis of these emission spectra using log-normal Gaussian components also suggested that the Trp environment was heterogeneous, with a major low-polarity component (~ 50–80%) and a component with higher polarity, close to that of an aqueous environment. This polar environment does not correspond to any of the environments experienced by the Pn model peptides. Thus, several positions and/or conformations within the micelle can be inferred for TM17 and mTM17, some of them not being observed for the model peptides.

The maximal quenching value of TM17 or mTM17 obtained in the presence of pure brominated detergent micelles (70–80%) is consistent with the contribution of the more hydrophobic component of the spectra. This component of the spectra may therefore be attributed to Trp into contact with the detergent acyl chain. However, the shape of the quenching curves (characterized by the lattice parameter *n*, reflecting quenching cooperativity) show that the Trp in TM17 or mTM17 is less accessible to detergent bromine atoms than that in Pn model peptides. Surprisingly, Trp was also clearly accessible to acrylamide (as

inferred from the bimolecular quenching constants k_q) such that adding the fraction of Trp accessible to acrylamide to that accessible to (brominated) acyl chains yielded more than 100%. These data may be interpreted as some Trp being accessible to both detergent chains and acrylamide. Detergent chains may fold back, so some quenching may occur within or close to the polar headgroup region. In addition, acrylamide accessibility is clearly not limited to a smooth surface around the micelle, because acrylamide somehow penetrates into the polar headgroup region, the extent of this penetration being smaller in DM than in DPC as judged from TOE fluorescence quenching in these micelles [32]. These results can be compared with those obtained in a detailed fluorescence study of various Trp mutants of the mechanosensitive channel MscL in a lipid model membrane: a clear and (opposite) dependence on Trp depth, of quenching by either a brominated lipid (di(9,10-dibromostearoyl-phosphatidylcholine)) or acrylamide [80] was observed. In this previous study, there seemed to be less overlap in quenching by brominated lipid and acrylamide for the Trp close to the membrane surface, consistent with more restricted dynamics of this system.

Time-resolved experiments provide additional clues. The homogeneity of the lifetime distributions of MRP1 fragments in neat solvents can be differently rationalized. Methanol is known as a promoter of peptide α-helix content which results in a major Trp conformer with a long lifetime. DMSO is more generally thought to favor a lack of secondary structure by disruption of intramolecular interactions [50] and may also specifically interacts with the indole ring, favoring a major conformer with the same lifetime as in MeOH [49]. In detergents, the lifetime distributions for MRP1 fragments and Pn peptides are more heterogeneous than in solvents, reflecting local conformer heterogeneity and less structure than in methanol. The lifetime distributions in the two detergents are also significantly different, being more heterogeneous in DM than in DPC. In particular, the amplitude of the longest lifetime, which is sensitive to the presence of α-helical structure [46], is reduced in DM as compared to DPC. This evidences a larger structural heterogeneity in the former than in the latter system. Moreover, the lifetime distributions of these MRP1 fragments do not exactly match any of those of model peptides. A significant trend was a smaller contribution of the longest lifetimes for MRP1 fragments with respect to model peptides, to the benefit of the intermediate lifetimes. This may indicate a less probable inclusion of Trp in an α-helix structure [46]. Significant nanosecond internal motion of the fragments within micelles was also evidenced, in particular in DPC, so that a same Trp may exhibit various degrees of accessibility to the water-soluble and micelle-bound quenchers during its lifetime. This situation may occur if the peptide inserts parallel to the micelle surface in the polar headgroup region and rotates on itself.

Such interfacial location is consistent with the results obtained in phospholipid vesicles, in particular the slight blue-shift of the emission spectrum with respect to that for the peptide in buffer. Time-resolved measurements in the presence of phospholipid vesicles were also performed (not shown) but where less reliable than in the optically clear micelles owing to the larger scattering of the liposomes.

Information about the overall structure of these fragments is provided by the CD experiments. Methanol promotes a highly α-helical structure (> 75% for mTM17), in agreement with numerous studies of hydrophobic and amphiphilic peptides. This high α-helix content matches the large amplitude of the longest lifetime in the solvents, which corresponds to the major *t* (*trans*) conformer in such secondary structure [46]. In contrast, mTM17 is much less helical in buffer. Interaction with detergent micelles induces significant structuring of the peptide (up to ~ 45% α-helix) as compared to buffer, but structuring remains less marked than would be expected for a peptide inserted radially within the micelle. In agreement with the lifetime distribution data, DPC exerts a stronger structuring effect than DM, as previously shown with fragments of a single-spanning membrane protein [41]. Together with the fluorescence data, these results suggest that the peptide is partly helical and located in the interfacial region of the micelle. They are also consistent with part of the sequence being composed of alternate hydrophobic and polar residues. CD does not indicate which regions of the peptide are structured, but secondary structure prediction programs (from www.predictprotein.org [81]) suggest that the structured part of the molecule lies within the Ser1235–Leu1247 sequence, which includes the Trp1246 residue at the edge of the helix. The rest of the peptide, in particular the hydrophobic stretch of 6 amino acids of the N-terminal fragment, is predicted to have no defined secondary structure.

Based on convergent results, we propose that the predicted TM17 fragment of MRP1 in the current topology model may behave, when isolated, like an amphiphilic peptide, resembling some antimicrobial peptides, such as those previously described [82–85] rather than a classical transmembrane segment. TM17 fragment is indeed the most amphipathic of all TM of MRP1 [9,86], and was not detected as a TM fragment in initial topology models. We suggest here that isolated TM17 mainly interacts with the interfacial region of the membrane, with no complete and stable (but maybe transient) insertion in a transmembrane orientation. The replacement of a neutral terminal residue by a charged residue (TM17/mTM17) appears to modify the depth of insertion with respect to the micelle surface slightly, as shown by the fluorescence quenching experiments. Within MRP1, TM17 might be driven to its transmembrane position by being linked to the rest of the protein and/or by its interaction with neighboring transmembrane segments (not necessarily the most proximal in the sequence). These opposite trends would give some plasticity to this protein domain that may undergo conformational changes of potential functional significance. This is in line with recent results from Ruysschaert et col. [87] providing evidence of TM segments motions for the whole protein during transport cycle. In addition, Trp_{1246} is a good candidate for being responsible of the overall changes that they observed in fluorescence quenching for reconstituted MRP1 upon binding of GSH alone, or with substrates and nucleotides. The behavior of TM17 is also reminiscent of previous observations for the transmembrane M6 fragment of Ca^{2+}-ATPase (SERCA1a), containing critical residues for calcium binding. The isolated M6 fragment was

shown not to have a high affinity for the membrane phase and was only partially structured [22,88]. This unconventional behavior of transmembrane domains may be the hallmark of membrane fragments involved in binding and transport. In a next step, study of the interaction of isolated TM17 with lipid model systems may strengthen our observations.

References

[1] S.P. Cole, G. Bhardwaj, J.H. Gerlach, J.E. Mackie, C.E. Grant, K.C. Almquist, A.J. Stewart, E.U. Kurz, A.M. Duncan, R.G. Deeley, Science 258 (1992) 1650–1654.
[2] R.G. Deeley, S.P. Cole, FEBS Lett. 580 (2006) 1103–1111.
[3] D.W. Loe, K.C. Almquist, R.G. Deeley, S.P. Cole, J. Biol. Chem. 271 (1996) 9675–9682.
[4] G. Rappa, A. Lorico, R.A. Flavell, A.C. Sartorelli, Cancer Res. 57 (1997) 5232–5237.
[5] H.J. Huh, C.J. Park, S. Jang, E.J. Seo, H.S. Chi, J.H. Lee, K.H. Lee, J.J. Seo, H.N. Moon, T. Ghim, J. Korean Med. Sci. 21 (2006) 253–258.
[6] C. Kast, P. Gros, J. Biol. Chem. 272 (1997) 26479–26487.
[7] C. Kast, P. Gros, Biochemistry 37 (1998) 2305–2313.
[8] D.R. Hipfner, K.C. Almquist, E.M. Leslie, J.H. Gerlach, C.E. Grant, R.G. Deeley, S.P. Cole, J. Biol. Chem. 272 (1997) 23623–23630.
[9] D.W. Zhang, S.P. Cole, R.G. Deeley, J. Biol. Chem. 277 (2002) 20934–20941.
[10] K. Ito, S.L. Olsen, W. Qiu, R.G. Deeley, S.P. Cole, J. Biol. Chem. 276 (2001) 15616–15624.
[11] J.D. Campbell, K. Koike, C. Moreau, M.S. Sansom, R.G. Deeley, S.P. Cole, J. Biol. Chem. 279 (2004) 463–468.
[12] J.L. Popot, D.M. Engelman, Annu. Rev. Biochem. 69 (2000) 881–922.
[13] D.M. Engelman, Y. Chen, C.N. Chin, A.R. Curran, A.M. Dixon, A.D. Dupuy, A.S. Lee, U. Lehnert, E.E. Matthews, Y.K. Reshetnyak, A. Senes, J.L. Popot, FEBS Lett. 555 (2003) 122–125.
[14] S.H. White, W.C. Wimley, Annu. Rev. Biophys. Biomol. Struct. 28 (1999) 319–365.
[15] P. Wu, C.J. Oleschuk, Q. Mao, B.O. Keller, R.G. Deeley, S.P. Cole, Mol. Pharmacol. 68 (2005) 1455–1465.
[16] X.Q. Ren, T. Furukawa, S. Aoki, T. Sumizawa, M. Haraguchi, Y. Nakajima, R. Ikeda, M. Kobayashi, S. Akiyama, Biochemistry 41 (2002) 14132–14140.
[17] B. de Foresta, L. Tortech, M. Vincent, J. Gallay, Eur. Biophys. J. 31 (2002) 185–197.
[18] E.J. Bolen, P.W. Holloway, Biochemistry 29 (1990) 9638–9643.
[19] I.B. Berlman, J. Phys. Chem. 77 (1973) 562–567.
[20] B. de Foresta, N. Legros, D. Plusquellec, M. le Maire, P. Champeil, Eur. J. Biochem. 241 (1996) 343–354.
[21] B. de Foresta, J. Gallay, J. Sopkova, P. Champeil, M. Vincent, Biophys. J. 77 (1999) 3071–3084.
[22] S. Soulié, B. de Foresta, J.V. Møller, G.B. Bloomberg, J.D. Groves, M. le Maire, Eur. J. Biochem. 257 (1998) 216–227.
[23] C.N. Pace, F. Vajdos, L. Fee, G. Grimsley, T. Gray, Protein Sci. 4 (1995) 2411–2423.
[24] J.V. Møller, M. le Maire, J. Biol. Chem. 268 (1993) 18659–18672.
[25] J. Lauterwein, C. Bösch, L.R. Brown, K. Wüthrich, Biochim. Biophys. Acta 556 (1979) 244–264.
[26] H. Zhang, A.S. Dvornikov, P.M. Rentzepis, J. Phys. Chem. A 109 (2005) 5984–5988.
[27] E.A. Burstein, S.M. Abornev, Y.K. Reshetnyak, Biophys. J. 81 (2001) 1699–1709.
[28] E.A. Burstein, V.I. Emelyanenko, Photochem. Photobiol. 64 (1996) 316–320.
[29] E. London, G.W. Feigenson, Biochemistry 20 (1981) 1932–1938.
[30] J.M. East, A.G. Lee, Biochemistry 21 (1982) 4144–4151.
[31] A.M. Powl, J.M. East, A.G. Lee, Biochemistry 44 (2005) 5873–5883.
[32] L. Tortech, C. Jaxel, M. Vincent, J. Gallay, B. de Foresta, Biochim. Biophys. Acta 1514 (2001) 76–86.
[33] M.R. Eftink, Methods Biochem. Anal. 35 (1991) 127–205.
[34] J.R. Lakowicz, Principles of Fluorescence Spectroscopy, Kluwer Academic Publishers, New York, 1999.
[35] M. Vincent, B. de Foresta, J. Gallay, Biophys. J. 88 (2005) 4337–4350.
[36] A.K. Livesey, J.C. Brochon, Biophys. J. 52 (1987) 693–706.
[37] J.C. Brochon, Methods Enzymol. 240 (1994) 262–311.
[38] Y.H. Chen, J.T. Yang, K.H. Chau, Biochemistry 13 (1974) 3350–3359.
[39] N. Sreerama, R.W. Woody, Anal. Biochem. 287 (2000) 252–260.
[40] N. Sreerama, S.Y. Venyaminov, R.W. Woody, Anal. Biochem. 287 (2000) 243–251.
[41] Y.M. Coïc, M. Vincent, J. Gallay, F. Baleux, F. Mousson, V. Beswick, J.M. Neumann, B. de Foresta, Eur. Biophys. J. 35 (2005) 27–39.
[42] D.B. Siano, D.E. Metzler, J. Chem. Phys. 51 (1969) 1856–1861.
[43] C.P. Pan, M.D. Barkley, Biophys. J. 86 (2004) 3828–3835.
[44] J.B. Ross, H.R. Wyssbrod, R.A. Porter, G.P. Schwartz, C.A. Michaels, W.R. Laws, Biochemistry 31 (1992) 1585–1594.
[45] A.G. Szabo, D.M. Rayner, J. Am. Chem. Soc. 102 (1980) 554–563.
[46] K.J. Willis, W. Neugebauer, M. Sikorska, A.G. Szabo, Biophys. J. 66 (1994) 1623–1630.
[47] S.L.C. Moors, M. Hellings, M. De Maeyer, Y. Engelborghs, A. Ceulemans, Biophys. J. (2006) biophysj.106.085100.
[48] M. Vincent, J. Gallay, A.P. Demchenko, J. Phys. Chem. 99 (1995) 14931–14941.
[49] E. Gudgin, R. Lopez-Delgado, W.R. Ware, J. Phys. Chem. 87 (1983) 1559–1565.
[50] M. Jackson, H.H. Mantsch, Biochim. Biophys. Acta 1078 (1991) 231–235.
[51] K. Kinosita Jr., S. Kawato, A. Ikegami, Biophys. J. 20 (1977) 289–305.
[52] B. Valeur, G. Weber, Photochem. Photobiol. 25 (1977) 441–444.
[53] Y. Chen, M.D. Barkley, Biochemistry 37 (1998) 9976–9982.
[54] D.R. Hipfner, R.G. Deeley, S.P. Cole, Biochim. Biophys. Acta 1461 (1999) 359–376.
[55] W.M. Yau, W.C. Wimley, K. Gawrisch, S.H. White, Biochemistry 37 (1998) 14713–14718.
[56] F.N. Petersen, M.O. Jensen, C.H. Nielsen, Biophys. J. 89 (2005) 3985–3996.
[57] J.A. Killian, G. von Heijne, Trends Biochem. Sci. 25 (2000) 429–434.
[58] T. Odahara, Biochim. Biophys. Acta 1660 (2004) 80–92.
[59] J.V. Møller, M. le Maire, J.P. Andersen, in: W. Pont, e.d. (Eds.), Progress in protein–Lipid interactions, Elsevier Science publishers BV, 1986, pp. 147–196.
[60] S. Lund, S. Orlowski, B. de Foresta, P. Champeil, M. le Maire, V. Moller, J. Biol. Chem. 264 (1989) 4907–4915.
[61] M. Jidenko, R.C. Nielsen, T.L. Sorensen, J.V. Moller, M. le Maire, P. Nissen, C. Jaxel, Proc. Natl. Acad. Sci. U. S. A. 102 (2005) 11687–11691.
[62] V. Mokhonov, E. Mokhonova, E. Yoshihara, R. Masui, M. Sakai, H. Akama, T. Nakae, Protein Expression Purif. 40 (2005) 91–100.
[63] W. Liu, Y. Kamensky, R. Kakkar, E. Foley, R.J. Kulmacz, G. Palmer, Protein Expression Purif. 40 (2005) 429–439.
[64] G.A. Scarborough, J. Exp. Biol. 203 (2000) 147–154.
[65] D. Stroebel, Y. Choquet, J.L. Popot, D. Picot, Nature 426 (2003) 413–418.
[66] R.K. Lytz, J.C. Reinert, S.E. Church, H.H. Wickman, Chem. Phys. Lipids 35 (1984) 63–76.
[67] T.J. McIntosh, P.W. Holloway, Biochemistry 26 (1987) 1783–1788.
[68] M.C. Wiener, S.H. White, Biochemistry 30 (1991) 6997–7008.
[69] R. Bader, A. Bettio, A.G. Beck-Sickinger, O. Zerbe, J. Mol. Biol. 305 (2001) 307–329.
[70] E. Schievano, T. Calisti, I. Menegazzo, R. Battistutta, E. Peggion, S. Mammi, G. Palu, A. Loregian, Biochemistry 43 (2004) 9343–9351.
[71] A. Dike, S.M. Cowsik, Biochemistry 45 (2006) 2994–3004.
[72] J.P. Powers, A. Tan, A. Ramamoorthy, R.E. Hancock, Biochemistry 44 (2005) 15504–15513.
[73] R. Estephan, J. Englander, B. Arshava, K.L. Samples, J.M. Becker, F. Naider, Biochemistry 44 (2005) 11795–11810.
[74] N. Sapay, R. Montserret, C. Chipot, V. Brass, D. Moradpour, G. Deleage, F. Penin, Biochemistry 45 (2006) 2221–2233.
[75] H.C. Ahn, N. Juranic, S. Macura, J.L. Markley, J. Am. Chem. Soc. 128 (2006) 4398–4404.

[76] J.T. Vivian, P.R. Callis, Biophys. J. 80 (2001) 2093–2109.
[77] D.P. Tieleman, D. van der Spoel, H.J.C. Berendsen, J. Phys. Chem. B 104 (2000) 6380–6388.
[78] T. Wymore, X.F. Gao, T.C. Wong, J. Mol. Struct. 486 (1999) 195–210.
[79] H. Khandelia, Y.N. Kaznessis, J. Phys. Chem. B 109 (2005) 12990–12996.
[80] A.M. Powl, J.N. Wright, J.M. East, A.G. Lee, Biochemistry 44 (2005) 5713–5721.
[81] B. Rost, G. Yachdav, J. Liu, Nucleic Acids Res. 32 (2004) W321–W326.
[82] A. Rozek, C.L. Friedrich, R.E. Hancock, Biochemistry 39 (2000) 15765–15774.
[83] W. Jing, A.R. Demcoe, H.J. Vogel, J. Bacteriol. 185 (2003) 4938–4947.
[84] R.M. Epand, H.J. Vogel, Biochim. Biophys. Acta 1462 (1999) 11–28.
[85] Z. Oren, Y. Shai, Biopolymers 47 (1998) 451–463.
[86] A. Seelig, X.L. Blatter, F. Wohnsland, Int. J. Clin. Pharmacol. Ther. 38 (2000) 111–121.
[87] C. Vigano, L. Manciu, J.M. Ruysschaert, Acc. Chem. Res. 38 (2005) 117–126.
[88] S. Soulié, J.M. Neumann, C. Berthomieu, J.V. Moller, M. le Maire, V. Forge, Biochemistry 38 (1999) 5813–5821.
[89] N. Rouvière, M. Vincent, C.T. Craescu, J. Gallay, Biochemistry 36 (1997) 7339–7352.